Earth and Space Science

Key Points:

- The convective heating is a major role in changing surface fluxes during drought and flood events
- The radiative imbalance plays a secondary role in determining drought and flood variability and its nature
- The elevated value of net incoming shortwave radiation would cause more severe drought than flood in near future

Correspondence to:
A. Maurya,
archana.maurya15@bhu.ac.in

Author Contributions:
Conceptualization: Archana Maurya, R. Bhatla
Data curation: Archana Maurya
Formal analysis: Archana Maurya, Shruti Verma, Manas Pant
Investigation: Archana Maurya
Methodology: Archana Maurya
Resources: Archana Maurya, R. Bhatla
Software: Archana Maurya
Supervision: R. Bhatla
Validation: Archana Maurya
Visualization: Archana Maurya, Shruti Verma, Manas Pant
Writing – original draft: Archana Maurya
Writing – review & editing: Archana Maurya, Shruti Verma, Manas Pant

Epochal Changes in the Intrinsic Nature/Dynamics of Flood and Drought During Indian Summer Monsoon

Archana Maurya[1], Shruti Verma[1], Manas Pant[1,2], and R. Bhatla[1,2]

[1]Department of Geophysics, Institute of Science, Banaras Hindu University, Varanasi, India, [2]DST-Mahamana Centre of Excellence in Climate Change Research, Institute of Environment and Sustainable Development, Banaras Hindu University, Varanasi, India

Abstract The basic and derived meteorological parameters, are important factors that affect the epochal changes of monsoonal drought/flood events which consequently influence the socio-economic aspects of India. The anomalous tricade departure of parameters namely rainfall, surface pressure, surface temperature, zonal and meridional wind, cloud cover (CC), outgoing longwave radiation, latent heat flux (LHF), sensible heat flux, net incoming shortwave radiation flux and net heat flux (NHF) have been considered between past, and recent tricade respectively drought and flood events. An anomalous decrease (-3 to -2 mm/d) in rainfall over the southern Arabian sea (AS), southern peninsular India and Bay of Bengal during past and recent tricade, on the other side increase (2–2.5 mm/d) in rainfall over the equatorial Indian ocean (EIO) during drought. The drought episode of the recent tricade is showing basin wise significant increase in LHF (20–30 W/m^2) and decrease in NHF (-30 to -60 W/m^2) from the Somali coast to Indonesian region which is linked with changing oceanic processes linked with the Indian ocean warming. The comparison of past and recent monsoonal flood has shown decrease in the CC over EIO and AS region which supported anomalous highest departure in LHF (12 W/m^2) over EIO. A direct association of dry and moist static energy variations have been found to be linked with the surface fluxes during Indian summer monsoon season. Further, epochal differences of vertically integrated moisture flux convergence is consistent with flood/drought rainfall anomaly. Thus, radiative imbalance also plays a secondary role in determining epochal nature of drought/flood variability and its nature.

Plain Language Summary The epochal variation of basic meteorological parameters and surface energy fluxes in monsoonal drought and flood episodes have been analyzed from 1961 to 2020. In this study, over the southern Arabian Sea (AS), southern peninsular India, and the Bay of Bengal decreasing rainfall during past tricadal monsoonal drought events while an increase in rainfall over the Indian Ocean (IO) has been observed by a change in the amount of cloud cover and surface energy fluxes. The undulating behavior of convective heating is associated with a significantly changing pattern of surface heat fluxes observed in past and recent monsoonal drought and flood episodes. Determining the epochal nature of drought and flood variability and its nature. The epochal departure in net incoming shortwave radiation flux is a considerable factor in contrasting dynamical features of drought and flood events along with monsoon circulation over the Indian region.

1. Introduction

The Indian summer monsoon (ISM) constitutes one of the most intense climatic elements, but its variabilities are mysterious (Rajeevan et al., 2000; Turner & Annamalai, 2012). The ISM has a stronghold, accounting for approximately 75%–80% of total annual rainfall of the country, thus plays a key role in the Indian agrarian system (Guhathakurta & Rajeevan, 2008; Parthasarathy et al., 1994; Trenberth et al., 2006). The ISM is characterized by considerable seasonal shifts in pressure, temperature, and winds, as well as changes in precipitation heavy rain during the monsoon season monsoon (Boos & Emanuel, 2009; Chakraborty & Agrawal, 2017; Goswami, 2006; Sikka & Gadgil, 1978). Because of differential heating landmass warm, sensible and latent heat is released from the land surface into the atmosphere, which drives the formation of low pressure. The monsoon flow is intensified by convective uplift as well as topographic forcing where mountains exist. These forcings and thermal gradients influence the strength, duration, and spatial distribution of large-scale monsoon systems (Dirmeyer, 1998; Webster et al., 1999; Xue et al., 2004). Therefore, land and ocean atmosphere interaction plays a crucial role in the monsoon systems (Fu et al., 2002). The ISM are large-scale phenomena that form an integral part of global-scale circulations and the circulation features are evident, bringing oceanic moisture inland. Meanwhile within those

circulations, the rainfall comes from moisture recycled over land from terrestrial evaporation (Sikka, 1980; Swain et al., 2009). These land surface fluxes provide a means for land-atmosphere interactions to modulate the monsoon (Narapusetty et al., 2016). Furthermore, Cadet and Diehl (1984); Krishnamurthy and Shukla (2007) studied that 70% of water vapor that crosses the western coast of India originates from the southern hemisphere and the rest 30% comes from evaporation over the Arabian Sea (AS).

Furthermore, numerous researchers have reported that the variation of ISM on a decadal to multidecadal scale contains a 60-year cycle (Krishnamurthy & Goswami, 2000). Pacific decadal oscillation and Atlantic multidecadal oscillation are different potential causes of the ISM rainfall (ISMR) decadal to multi-decadal scale variability (Bhatla et al., 2013, 2020; Malik & Brönnimann, 2018; Wang et al., 2018). The climatological mode remarkably modulates annual and seasonal variability. Several studies have recognized the interannual variability of monsoon rainfall over the last six decades (Joseph et al., 2009; Mooley & Parthasarathy, 1984). The rainfall study provides multiple possible outcomes such as linear trends, epochal variations, and teleconnections with the El Nino southern oscillation (ENSO) and the Indian Ocean Dipole (Gadgil, 2000; Krishnan et al., 2013; Sinha et al., 2015). Several studies investigated that changing in the land-sea thermal contrast may play an important role in weakening (strengthening) the intensity of the ISM and exhibits substantial seasonal, interannual, and decadal variability that results in severe droughts(floods) (Ding, 2007; Gu et al., 2020; Samson et al., 2017). It has also been found that land surface processes may play a significant role in these extreme events by regulating the heat gradient and moisture supply (Bhalme & Mooley, 1980; Ramesh et al., 2005; Xue & Shukla, 1993). A flood (drought) event in ISM is caused by a diverse range of phenomena in the oceans as well as land region. For illustration, ENSO is the most important and largest seasonal to interannual climate variation, and it has a major role on atmospheric circulation and precipitation over Asia, particularly in the summer season. Several studies have found that ENSO significantly affects the ISMR (Ashok & Tejavath, 2019; Hrudya et al., 2021; Varikoden et al., 2015). The ISMR has become relatively weak (stronger) all through establishing El Nino (La Nina) years, despite the fact that the negative relation between ENSO indices and ISMR must have weakened in recent epochs (Goswami & Chakravorty, 2017; Goswami et al., 2016; Todmal et al., 2022). Various investigations observed that floods have even more short active spells of the summer monsoon, although drought have long break spells (Rajeevan et al., 2010; Rajesh & Goswami, 2020; Vishnu et al., 2022). Certain endeavors have been made to diagnose the source of increased risk of longer break spells (Gadgil & Joseph, 2003). According to Goswami and Xavier (2003) and Rajeevan et al. (2010), the transformation from the break phase to the active phase is represented by quickly possible convective instabilities, that further consist entirely extensive of increased monsoon low-pressure behaviors in the active monsoon process.

The land surface fluxes allow land atmosphere connections to influence the monsoon system (Bhat, 2002; Bhatla et al., 2011; Mohanty & Dash, 1995; Mohanty et al., 1994). During the monsoon season multiple sets of rainfall pattern has decreased in South Asia over the last 5–6 decades (Annamalai et al., 2013). Monsoonal rainfall appears to be transferring from east to west (with increased rainfall over the tropical western Pacific (TWP) region and decreased rainfall across South Asia). The rising Sea surface temperature trend in the TWP has significantly changed atmospheric circulation, with even more dry and cold air advected over the northeast. The northward advancement of the ISM and moisture transport toward the Indian region is another aspect of an impact over the South China Sea as well as TWP dynamics (Vaid & Kripalani, 2021). Moisture inflow through the Indian western boundary has been utilized as a significant predictor for the ISMR and it plays major role in the inter-annual fluctuation of the ISMR (Ghosh et al., 1978; Levine & Turner, 2012; MP, 1983; Naidu et al., 2011; Nair et al., 2021; Sujith et al., 2017). The latitudinal differential pressure among both western Asia as well as the western equatorial Indian Ocean (EIO) can affect the strength of low-level moisture flux through the AS toward the Indian mainland (Chakraborty & Agrawal, 2017; Samson et al., 2017). The increased temperature over the western EIO is a considerable factor in decreasing monsoon circulation along with moisture advection over the Indian region (Roxy et al., 2014, 2015; Vishnu et al., 2016). Land surface processes, by modulating the heat gradient and moisture supply, might be playing an important role in these extreme weather events (Mahto & Mishra, 2020; Mishra et al., 2018). The interannual variation in all India averaged summer monsoon rainfall (AISMR) is small (Parthasarathy & Mooley, 1978; Shukla, 1987). Nonetheless, the socioeconomic consequences are massive, manifesting as catastrophic flooding and drought induced scarcity of water (Dhanya & Nagesh Kumar, 2009; Mishra et al., 2016). Such extremes conditions had an impact on India's foodgrain production as well as economic growth. An excess ISMR, results in severe floods, notably during the peak monsoon season months.

Table 1
Total Monsoonal Drought and Flood Events Using Indian Institute of Tropical Meteorology Rainfall Data During 1961–2020 (Past (T1) & Recent (T2) Epochs) Followed by Vishnu et al. (2022)

Time period	Drought	Flood
1961–2020	Total drought years (15 events)	Total flood years (8 events)
1961–1990 (T1)	1965, 1966, 1968, 1972, 1974, 1979, 1982, 1985,1986, 1987	1961, 1970, 1975, 1983, 1988
1991–2020 (T2)	2002, 2004, 2009, 2014, 2015	1994, 2007, 2019

The spatial and temporal variation of ISMR is influenced by a variety of climatic and geographical characteristics throughout the Indian subcontinent (Gadgil, 2000; Goswami et al., 2003; Parthasarathy et al., 1994). Bingyi (2005), Singh and Borah (2013), Joseph & Simon (2005) used different data sets to confirm the long time series of ISMR deviates from a normally distributed pattern, with a deviation toward drought. In this study first we have discussed the average climatology with average of all monsoonal drought and flood events rainfall for basic parameters such as: rainfall, surface temperature and wind. Along with the average of past, and recent and their differences in monsoonal drought (deficient rainfall years) and flood events (excess rainfall years) are presented. The intensity of AISMR is dependent on the amount of moisture supplied to the landmass by low-level winds. An excess AISMR, brought serious floods, during the peak summer monsoon months. When the AISMR anomaly is below 10% (more than 10%) of its long-term mean, monsoonal droughts (floods) arise. Droughts (floods) are identified by a stronger (relatively weak) meridional pressure gradient over the Northern Indian Ocean, a less (more) northward seasonal movement in the monsoon trough, a high (low) frequency of monsoon depressions with an extended (short) westward path (Bhalme & Mooley, 1980; Goswami & Ajaymohan, 2001; Vishnu et al., 2020). The objective of this study is to analyze the contrasting features of monsoonal drought and flood events to understand that how it affects both temporally and spatially in different geographical regions. Regardless of the significance of monsoonal systems in supplying irrigation water for agriculture the impact of land/atmospheric interactions in the monsoon system remained unclear. As a possible consequence, remarkably asymmetric ISM events like drought and flood could have a disastrous impact on crop production and management of water resources.

2. Data and Methodology

In this study, the variability of certain basic and surface meteorological parameters with the components of the net heat fluxes are studied for the selected monsoonal drought and flood events during the summer monsoon season. The selection of monsoonal drought (rainfall deficient) and flood events (rainfall excess) with the help of Indian Institute of tropical meteorology rainfall data, assembled by Parthasarathy et al. (1994) from the website: http://www.tropmet.res.in during 1961–2020. Furthermore, the AISMR during a given year is deficient(excess) by less(more) than 10% of the climatological normal daily data is used to calculate monsoonal drought and flood during the period of 1961–2020 (Vishnu et al., 2022). There are two tricades such as; past (T1; 1961–1990) and recent (T2; 1991–2020) with 15 monsoonal droughts as well as 8 flood events shown in Table 1. The spatial distribution of mean climatology, monsoonal drought (rainfall deficient), and flood events (rainfall excess) for these basic parameters play a significant role in understanding the changing pattern of monsoonal flood (drought) events.

The reanalysis data sets from National Centre for Environmental Prediction/National Centre for Atmospheric Research Reanalysis (NCEP/NCAR) at 2.5° × 2.5° horizontal resolution provides a consistent and reliable data set to investigate the contrasting feature of monsoonal drought and flood events along with associated energy fluxes in changing climate. The NCEP reanalysis data plays an important role in understanding the climate system and also helps in examining the variation of basic and surface meteorological parameters for average monsoonal drought and flood events over the Indian region (40°N–10°S & 20°E−110°E). The global reanalysis data sets are available at http://www.cdc.noaa.gov/cdc/data.ncep.reanalysis.surface.html (Kalnay et al., 1996) and are preferred over other reanalyzes data as it offers a longer period of availability. These data sets have been generally used in several spatiotemporal climate studies (Bhatla et al., 2022; Sahana et al., 2015; Yanai & Tomita, 1998). The mean daily reanalysis parameters such are rainfall, surface pressure, surface temperature, wind (zonal & meridional), cloud cover (CC), Latent heat Flux (LHF), Net outgoing longwave Radiation Flux

(NLWRF), Net incoming shortwave radiation flux (NSWRF), and net heat flux (NHF). In this analysis, average epochal changes of monsoonal drought and flood events have been studied using the reanalysis data sets. The variation in sensible heat flux (SHF) over land and oceanic regions are less prominent as compared with other fluxes and used in the calculation of NHF. Furthermore, NHF is calculated from these data sets based on the following equation:

$$NHF = NSWRF - (NLWRF + LHF + SHF) \qquad (1)$$

Along with temporal tricadal departure of land and oceanic surface fluxes over selected regions during drought (flood) event. The significant changes are observed over the selected regions such as all India land region (AI), central India (CI; 74°E−75°E, 20°N−27°N), southern peninsular India (SPI; 75°−80°E, 8°−18.5°N), Arabian sea (AS; 55°E−73.5°E, 8°N−20.5°N), Bay of Bengal (BoB; 81°E−94°E, 7°−18°N), equatorial Indian ocean (EIO; 48°E−98°E, 7°S−5°N), and southern Indian ocean (SIO; 50°E−108.5°E, 29°S−10°S). In this analysis, the positive sign of NHF represent more energy flux is coming in (heating or source region) although negative NHF more energy going out (cooling or sink region) from the surface (Bhatla et al., 2011; Mohanty et al., 1996; Rahul & Gnanaseelan, 2016).

Further to analyze the thermodynamic features of monsoonal drought and flood episodes, we have calculated dry static energy (DSE), moist static energy (MSE) and vertically integrated moisture flux convergence (VIMFC). The (DSE) and (MSE) is derived from the first law of thermodynamics and has been widely used over tropical region because of its energetic, stability of atmosphere and conventionally recognized conservation properties (Nanjundiah & Srinivasan, 1999; Pillai & Sahai, 2014), mathematically written as:

$$\text{Dry Static Energy (DSE)} : d = CpT + gz \qquad (2)$$

$$\text{Moist Static Energy (MSE)} : h = CpT + gz + L_v q \qquad (3)$$

Where d is DSE, h is MSE, Cp is the specific heat capacity at constant pressure (1,004 J/Kkg), T is temperature (K), g is acceleration due to gravity (9.8 ms^{-2}), z is the geopotential height (m), Lv is the latent heat of vaporization (2.5 × 10^{6}Jkg^{-1}), and q is the specific humidity. The VIMFC is calculated to determine the changes in atmospheric moisture convergence/divergence over India (Trenberth & Guillemot, 1998) and given as:

$$\text{VIMFC} = -\nabla \cdot \frac{1}{g} \int_{1000}^{300} qV \, dp \qquad (4)$$

Where V is the wind velocity vector, ∇ is the gradient operator, and q is the specific humidity, and integrated over surface (1,000 hPa) to the top of the atmosphere (300 hPa) with respect to pressure.

Here we have applied the statistically significant t values at 95% level of significance and contoured (blue line) in epochal changes of monsoonal drought and flood events using different basic and surface meteorological parameters.

3. Results and Discussion

The spatio-temporal variations of different meteorological parameters during the monsoonal flood and drought events over India have been discussed. For that purpose, the three time slices defined as long-term mean (60 years; 1961–2020), past (T1; 1961–1990) and recent tricades (T2; 1991–2020). The distribution patterns of rainfall, surface wind, and temperature during the long-term mean (climatology) along with selected monsoonal drought and flood events (Table 1) have been illustrated in Figures 1a–1i The higher intensity of mean rainfall (10–12 mm/day) over EIO, AS, BoB, Western ghats (WGs), North East (NE), West Bengal, and its adjoining region have been reported as far as Indian landmass is concerned during the long period (Figure 1a). A deficiency in rainfall (2–3 mm/day) over EIO, AS, WGs, SPI, CI, north India (NI), and Western India (WI) during composite monsoonal drought years while excess rainfall during flood years over these regions have been reported (Figures 1b and 1c). In addition, Figures 1d–1f depicted the spatio-temporal distribution of wind vector magnitude of composite climatology, monsoonal drought, and flood events. The southwest movement of low-level cross-equatorial winds over the Indian Ocean (IO) and westward flow over the subcontinent and the adjoining AS and BoB can be noticed (Figure 1d). Also, maximum wind speed (more than 10 m/s) near Somali coast low-level jet (LLJ) wind propagates into AS branch and BoB branch cover entire Indian region during ISM (June, July, August, September; JJAS) period. Due to the presence of a huge amount of moisture energy by convective heating
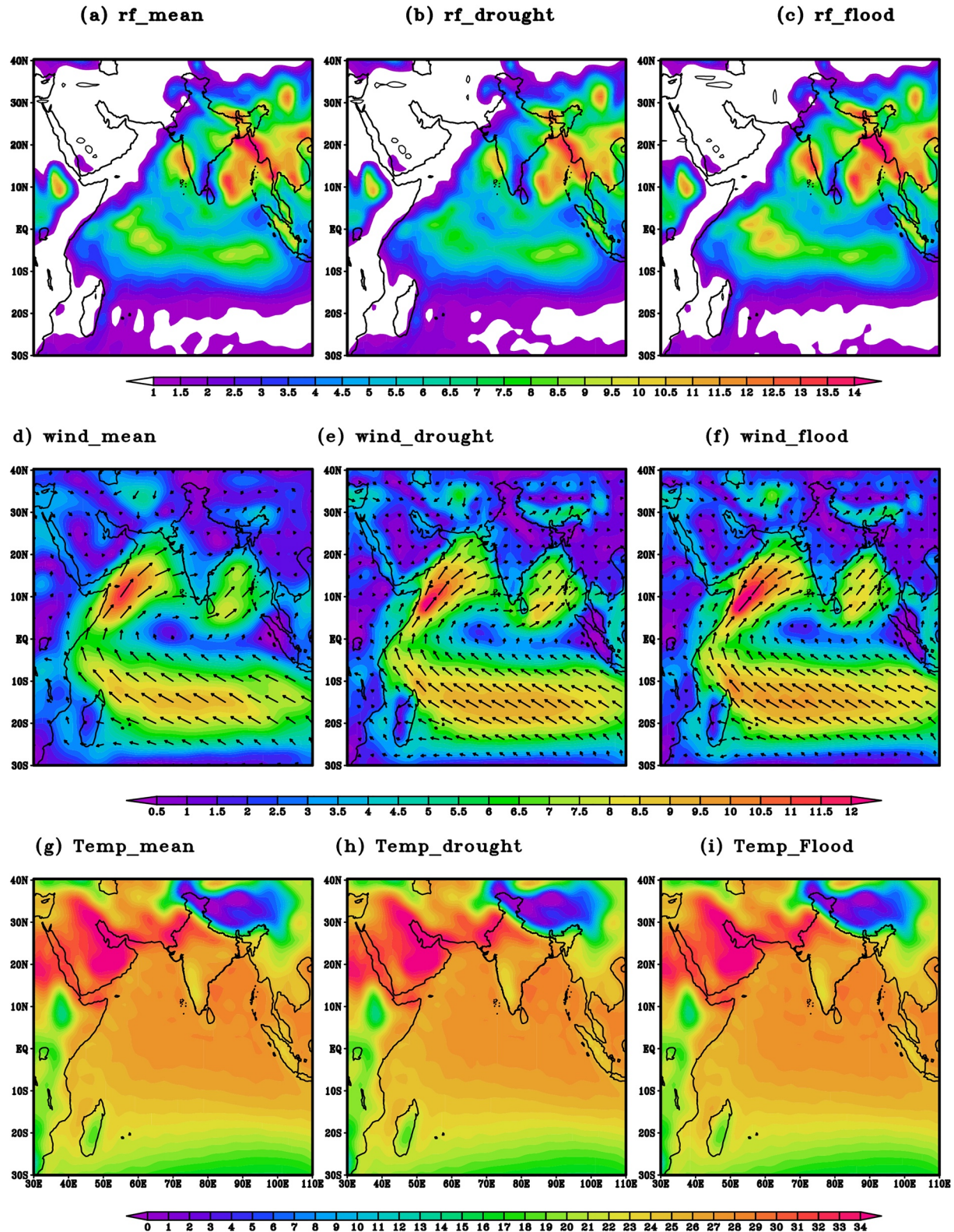
Figure 1. (a)–(i) Climatological and epochal (Tricadal) distribution for different drought and flood events overall India of average rainfall, wind, and Temperature using National Centre for Environmental Prediction reanalysis data for June–September (JJAS) from 1961 to 2020 (a) mean distribution of average rainfall (mm/day); (b)–(c) mean distribution of average drought (rf_drought; 15 events) and flood events (rf_flood; 8 events); (d)–(f) and (g)–(i) same as (a)–(c) but for wind (m/s), and surface temperature (°C) respectively.

and LLJ a higher wind speed over the oceanic region than land region during the ISM season have been observed. Further, the average wind circulation gets strengthen over Mascarenes and Somali coast during flood events than the drought events and however, follows a similar pattern of average rainfall distribution (Figures 1e and 1f). The distribution pattern of surface temperature shows very slight variation during long-term climatology, monsoonal drought and flood years. However, over the SIO lesser surface temperature has been reported which substantially increases toward the northern region due to the shifting of intertropical convergence zone in the northern hemisphere during monsoon season (Sikka & Gadgil, 1980; Xu et al., 2019). However, the maximum surface temperature is found western part of the Indian region and its adjoining region. Similarly, minimum surface temperature has been observed over Himalayan and Tibetan plateaus due to topographical structure at higher altitudes. Several studies found that the ISM is intense over the oceanic region and most active over the AS, BoB as well as IO and propagates over land region (Joseph et al., 2006; Krishna & Rao, 2008).

3.1. Spatio-Temporal Variation of Basic Meteorological Parameters During Drought Events of AISM

Figures 2a–2i represents the spatial variation in rainfall, surface pressure and temperature during all India monsoonal drought years. The spatial distribution of past (T1), recent (T2), and their differences (T2-T1) for these basic parameters might play a significant role to understand the contrasting pattern in monsoonal drought and flood events. Figures 2a–2c depicted the variation in rainfall for all of India's monsoonal drought events. The intensity of rainfall increases over CI whereas decreasing pattern observed over WGs (−1.5–3 mm/day), a major part of SPI (−0.5 to −2.5 mm/day), AS (−2–3.5 mm/day) and BoB (−1 to −3.5 mm/day) T2 as compared to T1. There is an enhancement in rainfall intensity over EIO (1–4 mm/day) during recent epoch (Figure 2c) and the blue contour lines represent statistically significant at 95% confidence level. Similarly, a decreasing pattern observed for surface pressure over most of the Indian land and oceanic region except upper northern India along with WI, western AS (WAS), western IO (some positive value about 0.5–2 hPa, Figure 2f). Also, surface pressure is relatively high in the northern IO in past and recent monsoonal drought events. The distribution of Surface temperature and their differences are also depicted in Figures 2g–2i and statistically significant at 95% confidence level in blue contour lines. As far as surface temperature is concerned, a substantial rise over CI, SPI, IO, BoB (most of the region in recent tricade), while slightly negative values (decrease) have been observed over some parts of WI, upper NI, and NEI. These results agree with Kothawale et al., 2008 and May (2004), indicate the impact of heating due to land and ocean contrast energy fluxes. A comparison of these features brings out the difference in circulation over the selected regions.

The composite analysis of all India monsoonal drought events for wind, CC, and OLR distribution is depicted in Figures 3a–3i. Considering the cross-equatorial flow, it is observed that the variations are much prominent over AS than the BoB region which does not supports the significant variability over BoB (Figures 3a and 3b). Strengthening in wind pattern (0.5–1 m/s) over AS and SIO during recent tricadal drought events (T1) than past (T2) monsoonal drought events have been reported (Figure 3c) and contoured regions are statistically significant above 95% confidence level. However, a slight enhancement (0.2–0.8 m/s) over entire Indian landmass and BoB has been observed and also, a strong wind gradient can be observed over the EIO. The differences of wind speed over AS, BoB, and WIO has been considered the most energetic region in the tropics (Walker cell). Webster (1981) summarized that wind anomalies on the western side of the source are stronger than those on the eastern side. However stronger cross-equatorial flow is observed around 50°E and with higher intensity during past as well as recent monsoonal drought years. The spatial distribution of CC during T1 events has been found to be dominant than T2 over BoB, EAS, and SPI (about 60%–70%) as compared to other regions of interest which can also be seen as negative difference (decrease of −5% to −10%) and statistically significant with student's t-test at 95% level (Figure 3f). Further, the major enhancement in CC has been observed over SIO (10%–20%) in the recent tricade T2 due to increase in surface temperature, wind strength and solar heating. The distribution of CC and its anomalies during the summer monsoon season for drought T1 & T2 follow the same pattern as the surface winds for the corresponding periods over the IO. This is because the genesis of CC over the warm tropical oceans is mainly due to convective activity triggered by strong surface winds, turbulent transport, and frictional convergence of moisture in the marine boundary layer (Mishra et al., 2016; Yasunari, 1979). Also, the differences of CC between the past and recent monsoonal drought events depict a decline (−2% to −8%) all over the ocean and land region except SIO (10%–20%) and WAS (6%–10%). Similarly, the spatial distribution of OLR for all Indian monsoonal drought events is depicted in Figures 3g–3i. The positive variations in OLR have been observed over all India land and oceanic region (above 4 W/m^2) except some parts of WI, NI, and NEI (−2 to
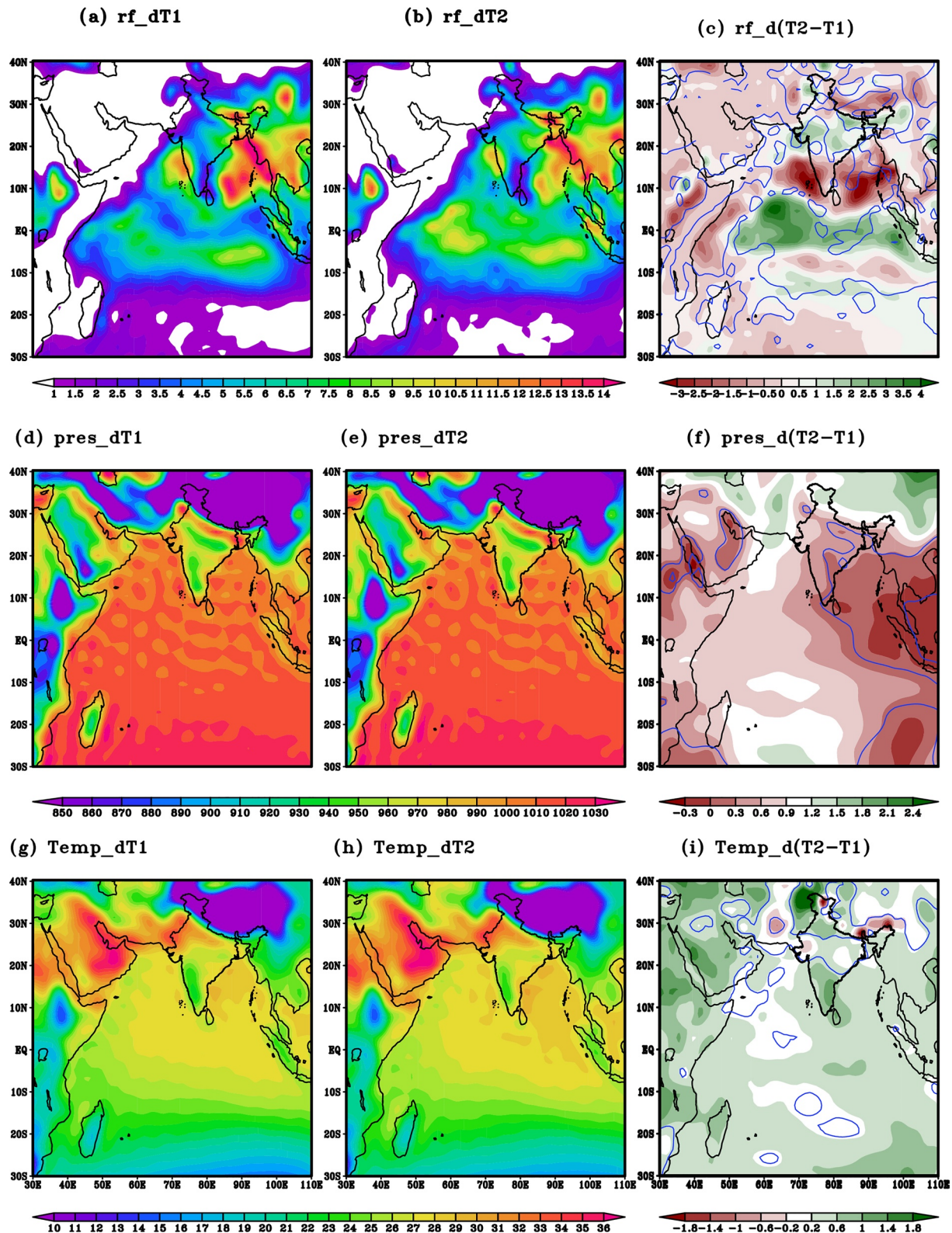
Figure 2. (a)–(i) Composite distribution of average drought and flood events over all India using National Centre for Environmental Prediction reanalysis data for June–September (JJAS) from 1961 to 2020 for (a) and (b) average distribution of rainfall (mm/day) drought events for past tricade (T1; 1961–1990) and recent tricade (T2; 1991–2020); (c) difference between recent and past tricade (T2-T1); (d)–(f) and (g)–(i) same as (a)–(c) but computed for surface pressure (hPa) and surface Temperature (°C), respectively. Blue contours in epochal changes of (c), (f), and (i) manifests the statistically significant regions above 95% confidence level by student's T test.
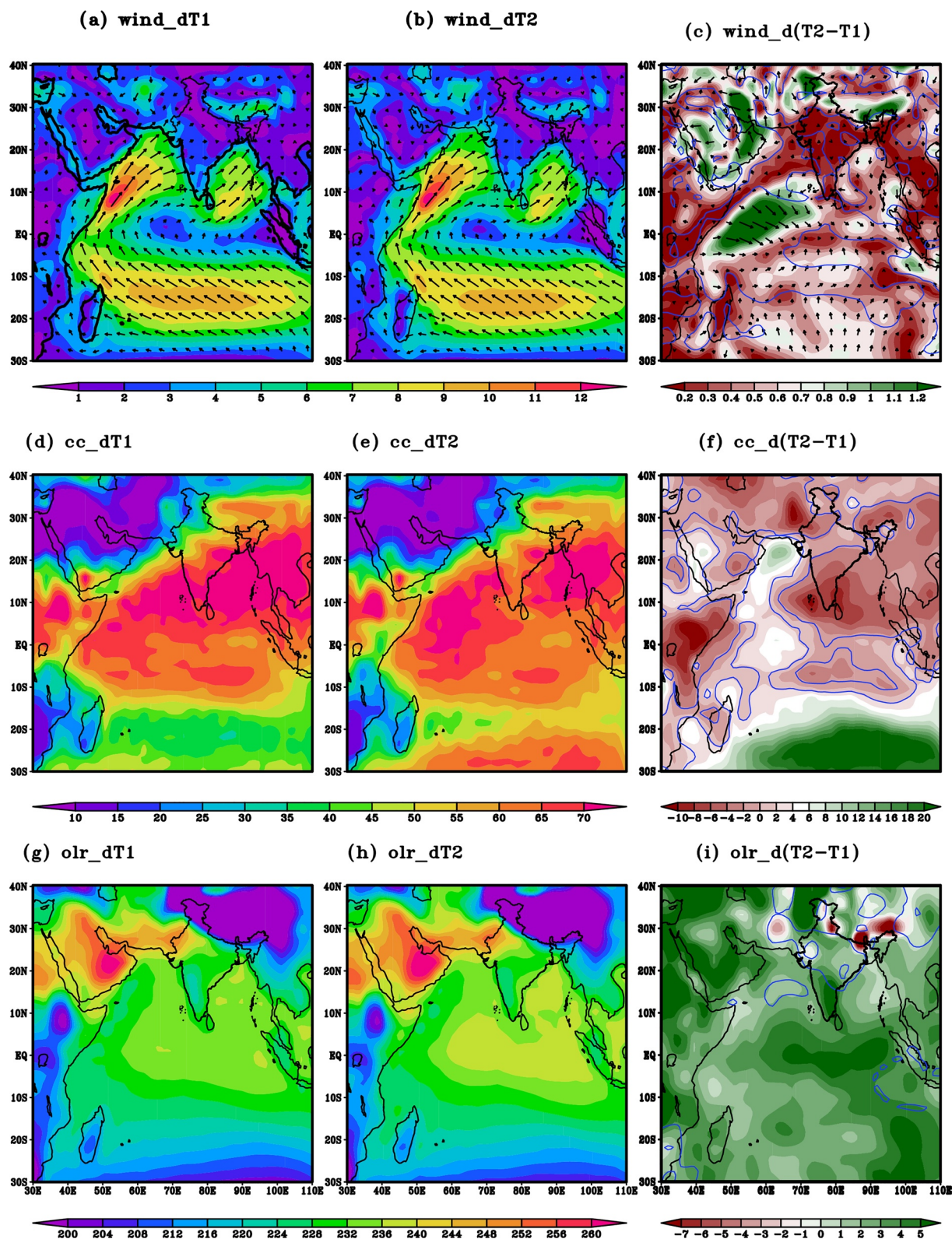
Figure 3. (a–i) Same as Figure 2 but computed for drought events of wind (m/s), cloud cover (%) and outgoing longwave radiation (W/m²).

-5 W/m^2). Several researchers analyzed, the distribution of OLR has a major role to the earth's energy budget and helps in regulating the processes such as evaporation and moisture during ISM season (Gadgil et al., 2003; Trenberth & Stepaniak, 2004).

3.2. Spatio-Temporal Variation of Surface Fluxes During Drought Events of AISM

The changes in surface fields during 1961–2020 are discussed in association with the monsoonal drought events. The magnitudes of the NHF, SHF, and OLR flux are found to be considerably less than the NSWRF and the LHF. The surface fluxes contribute toward the oceanic and land heat loss (gain) such as the LHF, NSWRF, and NHF during summer monsoon season in T1 and T2 as well as their differences (T2-T1) for all India monsoonal drought events represented in Figures 4a–4i. The average LHF of all India monsoonal drought events in T1 more-over the oceanic region such as the SIO, AS, BoB (180–240 W/m^2) during monsoon season due to strong Somali jet and stronger trade winds. In contrast, there is decreasing pattern of LHF over SIO, eastern AS (EAS), WGs, BoB, and the adjoining region of WGs with some parts of PI and CI during T2 (Figure 4b). On the other hand, Figure 4c depicted the differences between past and recent tricades over all of India's monsoonal drought events and statistically significant at 95% level in blue contour lines. The large negative value of LHF is found over AS (-30 to -50 W/m^2) and BoB (-20 to -30 W/m^2). Similar distribution for NSWRF in Figure 4d found minimum over SIO (-120 to -150 W/m^2), BoB (-140 to -160 W/m^2), some parts of SPI (-160 W/m^2), and West Bengal (-160 to -170 W/m^2) meanwhile the rest part enhanced in magnitude. The average distribution of NSWRF for monsoonal drought events during the recent epoch (T2) has a large value observed over EAS, BoB, and all Indian land regions except the NEI region (Figure 4e). It is also observed in Figure 4f a positive anomaly statistically significant at 95% level (blue contour lines) over upper SIO (3–12 W/m^2), EIO, WAS, and some parts of the NEI region, meanwhile a negative anomaly is observed over EAS, BOB, SPI, CI, and WI (-3 to -15 W/m^2). Along with the simple mean distribution of NHF for all India monsoonal drought events (1961–2020), past (T1), and recent epoch (T2) are also depicted in (Figures 7g–7i). In this analysis, the region's positive net radiation means that the regions where more energy flux is coming in than going out (most part of land region, upper WGs, head BoB, and some part of EIO) while negative net radiation means that the regions where more energy is going out than coming in are dark red to whitish red in color (SOI, AS, BoB). The spatial distribution of NHF for all of India's average monsoonal drought events (Figure 4g) and past epochal (Figure 4h) found almost similar patterns over the oceanic region (negative NHF) such as SIO (-60 to -100 W/m^2), AS (-20 to -30 W/m^2), BoB (-30 to -40 W/m^2) and land region (positive NHF) whereas EIO region having some positive NHF (10–20 W/m^2). Further in the recent epoch (Figure 4i), the strengthening of net incoming energy over the oceanic region as SIO (-30 to -90 W/m^2) and extension of negative net radiation over some part of EIO (-10 to -30 W/m^2), BoB (-30 to -50 W/m^2), AS (-20 to -40 W/m^2). The positive net radiation observed over all India land region (10–30 W/m^2) and increases over upper NI (30–40 W/m^2) except WGs, SPI. It is clearly observed that the variation in surface heat fluxes is found over oceanic regions (more) as well as land regions (less) except SPI. The NSWRF value shows significant positive departure over SPI and BoB (above 15 W/m^2), on the other hand over AS, EIO, SIO having negative departure about -10 W/m^2 from recent to past monsoonal drought events (Figure 4j). However, the maximum departure in LHF found over EIO (18 W/m^2), slightly decreases over AS & SIO (10 W/m^2) and minimum departure over BoB (-2 W/m^2) (Figure 4j). Several diagnostic studies found that the atmospheric and oceanic components exchange daily averaged quantities such as heat energy and momentum fluxes during ISM season (Mohanty & Mohan Kumar, 1990; Mohanty & Ramesh, 1993, Mohanty et al., 1996).

3.3. Spatio-Temporal Variation in Thermodynamic Features During the Drought Events of AISM

The thermodynamic features such as DSE, MSE and VIMFC have been analyzed during drought episodes during different epochs (Figures 5a–5i). Since wind circulation associated with monsoon is primarily responsible for the rainfall variability and moisture transport along-with that the MSE plays a secondary role as well as the variations of MSE are directly linked to the surface energy fluxes as MSE is influenced by wind-driven components of surface LHF (Neelin, 2007). Figures 5a–5c, depicted the spatio-temporal variation of DSE in T1 and T2 and their differences in composite monsoonal drought events. Since DSE is conserved during unsaturated vertical and horizontal motion in the atmosphere and similar to potential temperature. There is an increasing pattern of DSE from ocean to land region in the order of 298–310 kJ/kg during past and recent monsoonal drought episodes due to the higher specific heat capacity of land as compared to the ocean. There are some departures observed in epochal changes of DSE (Figure 5c) and contoured regions are significant above 95% confidence level by
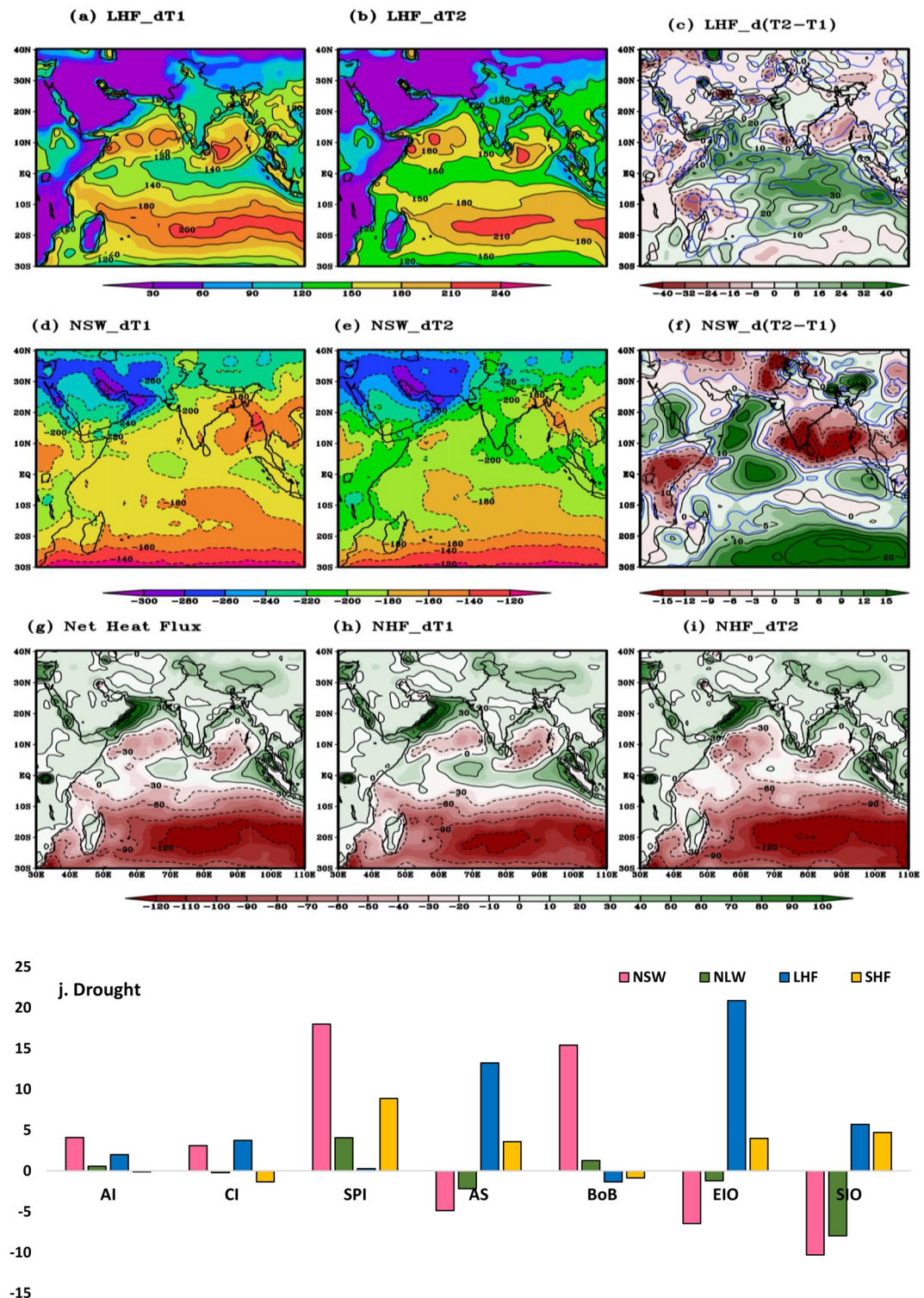
Figure 4. (a–i) Same as Figure 2 but computed for drought events of latent heat flux (W/m^2), net incoming Shortwave radiation (W/m^2) and net heat flux (NHF; W/m^2), (g) average NHF of (h) past and (i) recent tricade for all monsoonal drought events (j) temporal tricadal departure of land surface fluxes over selected regions during drought event.

student's t test. The positive increment of DSE in recent tricade cover maximum land and oceanic region except some parts of lower AS, Mascarenes region and eastern side of SIO. Similarly, the spatial distribution of MSE illustrated in Figures 5d–5f and increases in recent tricade over WI, NI, NEI, some parts of SPI, AS, BoB, EIO,
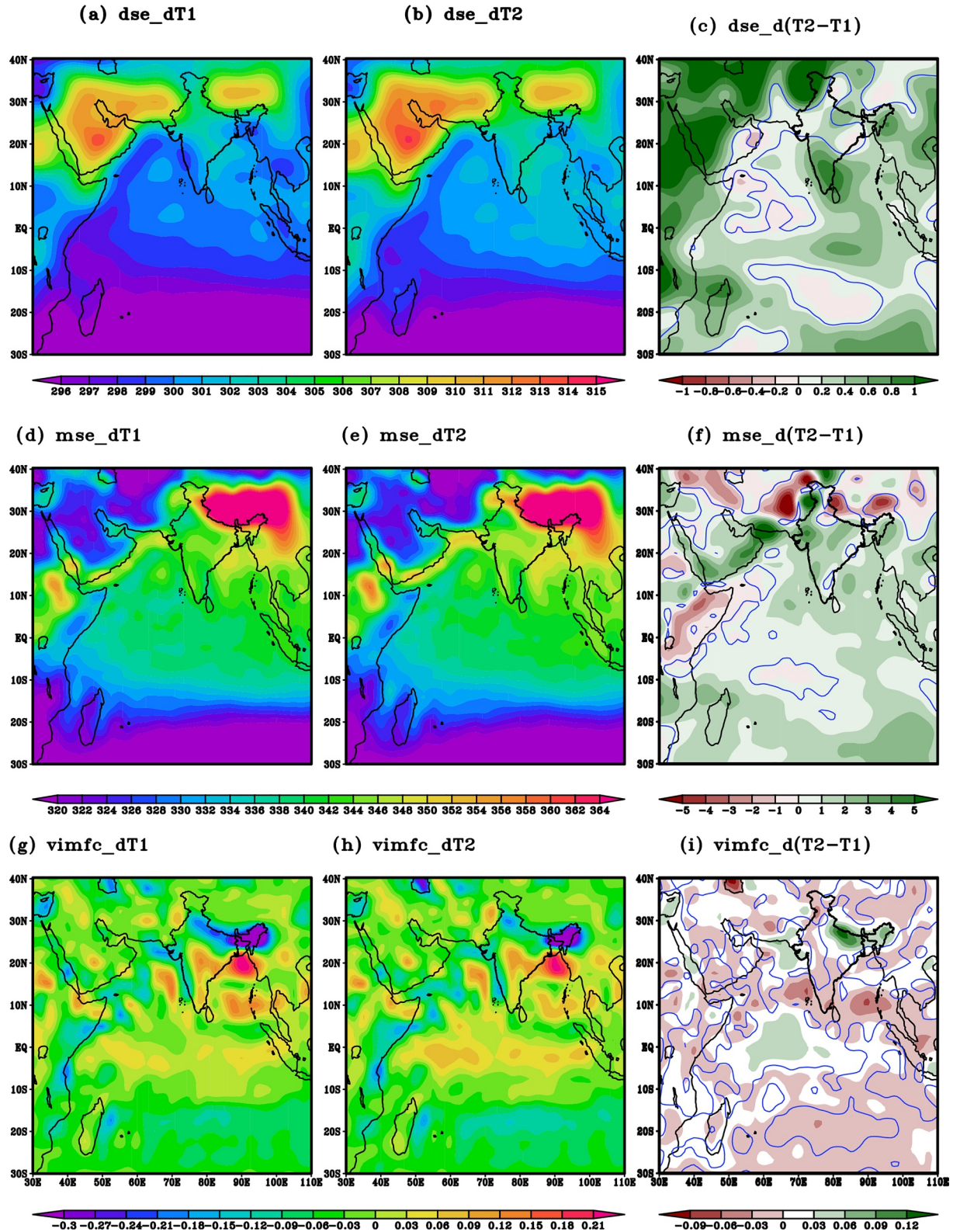
Figure 5. (a–i) Same as Figure 2 but computed for drought events of dry static energy (kJ/kg), moist static energy (kJ/kg) and vertically integrated moisture flux convergence ($10^{-5} \text{kgm}^{-2}\text{s}^{-1}$).

and western SIO, although diminished over eastern SIO. The epochal differences of MSE for composite drought episodes, it is observed that BoB branch is stronger than AS branch during drought events of ISM in the order of 0.2–0.6 kJ/kg for DSE and 1–2 kJ/kg for MSE. Further the VIMFC are calculated to determine the changes in atmospheric moisture convergence/divergence over India (Mishra et al., 2020). The positive value of VIMFC manifests the convergence region whereas a negative value of VIMFC is divergence region. During monsoonal drought events, maximum convergence region was observed over BoB than AS region due to a strong moisture flux energy further convergence region also observed over EIO due to enhanced heating over the region. The epochal differences of VIMFC have been depicted in Figure 5i, there are enhancements in recent tricade over eastern EIO, northern AS, NI and NEI in the order of 0.03–0.9 × 10⁻⁵ kg/m²s while the rest of the regions having reported decreasing VIMFC in the order of −0.03 to −0.06 × 10⁻⁵ kg/m²s. Also, a decreasing VIMFC pattern over SIO, southern AS, southern BoB, SPI, and some parts of WI have manifested severe droughts during the recent tricade.

3.4. Spatio-Temporal Variation of Basic Meteorological Parameters During Flood Events of AISM

Prior to a large excess rainfall season over India, a significantly warmer oceanic region exists over the north AS close to the northwest coast of India during the monsoon season. However, during the ISM season, surface pressure anomalies do not display any significant variations between the two extreme categories of the monsoon (flood as well as drought). Figures 6a–6i represent the spatial variation of rainfall, surface pressure, and temperature during all Indian monsoonal flood events. The spatial distribution of past (T1), recent (T2), and their differences (T2-T1) for these basic parameters play a major role to understand the contrasting pattern in monsoonal flood events. Figures 6a–6c depict the variation in rainfall for all Indian flood events during the monsoon season. The intensity of rainfall increases over CI while decreasing pattern has been observed over WGs (−1.5–3 mm/day), the major part of SPI (−0.5 to −2.5 mm/day), AS (−2–3.5 mm/day) and BoB (−1 to −3.5 mm/day). In the recent epochs (Figure 6c) there is a strengthening in rainfall over EIO (1–4 mm/day) and significant with student's t-test at 95% level. Similarly, there is a decreasing pattern observed for surface pressure (Figures 6d–6f) over most of the Indian region except western and upper northern India along with BoB, and eastern IO, whereas some positive value of surface pressure is found over western IO. However, surface pressure anomalies have less significant variations between the two T1 and T2 of monsoonal flood events over land regions (Figures 6d–6f). The distribution of Surface temperature and their differences are also depicted in Figures 6g–6i. There is an increase in temperature recent (T2) flood events as compared to the past (T1) during ISM season. As a result of changing climate, the enhancement in surface temperature (0.5–1.5°C) has been observed over SPI, some part NEI, BoB, EAS, WEIO, and SIO though slight decline over NI, WAS, and some parts of eastern SIO in the range of −0.5 to −1.5°C. Similarly, the composites of wind, CC, and OLR distribution during flood years have been illustrated in Figures 7a–7i for the period T1, T2, and (T2-T1) during flood events. The strengthening in wind speed over AS, EIO, and some isolated parts of Mascarenes and BoB has been observed during T2 than in past T1 (Figures 7a–7c). It is clear from Figure 6c, in the recent epochs the wind strength has been decreased over the land regions as well as central SIO during ISM season and significant at 95% level. The spatial variation of wind patterns can be understood with the help of CC distribution (Figures 7d–7f). In the recent epochs, there is an enhancement in the spatial variation of CC over land regions following a similar wind pattern. However, variation of CC more than 70% can be observed over the oceanic regions mainly SIO, EIO, and WGs (Figure 7e). The major positive differences of CC are found over SIO (15%–20%) (Figure 7f) during ISM flood years. Further, the spatial distribution of OLR for all Indian monsoonal flood events is depicted in Figures 7g–7i statistically significant with student's t-test at 95% level in blue contour line. It is clear from Figures 7g and 7h, a maximum value of OLR is observed over WI and its adjoining regions (240–255 W/m²) as well as over centre of EIO (240–250 W/m²) while lesser (220–230 W/m²) have been reported over SPI, WAS, and SIO. Similarly, major parts of CI having OLR in the order of 240–245 W/m². There are more positive OLR variations observed over land and oceanic region (T2-T1; 2–7 W/m⁻²) as in Figure 7i. However, the negative departure is observed in OLR over some parts of Upper NI, NE, and eastern SIO region (−1 to −6 W/m²) during ISM season.

3.5. Spatiotemporal Variation of Surface Fluxes During Flood Events of AISM

The composite distribution of surface heat fluxes namely; LHF, NSWRF, and NHF during the ISM flood years in past and recent tricades have been shown in Figures 8a–8i. The maximum values of LHF (180–240 W/m²) during past flood events (Figure 8a) found to be dominant over oceanic regions such as SIO, AS, and BoB which is attributed to the strong Somali jet and stronger trade wind in the southern hemisphere. Further, in recent
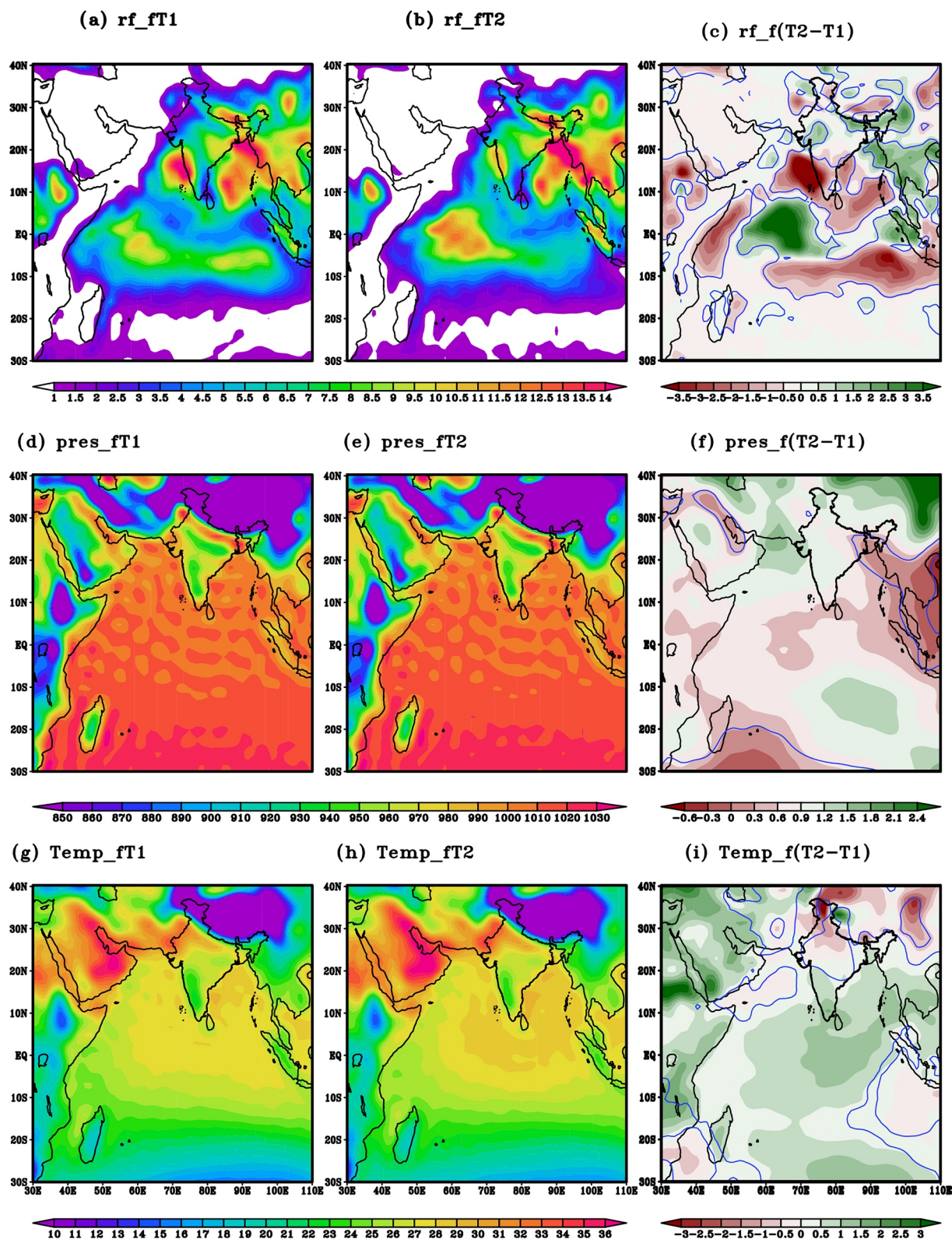
Figure 6. (a–i) Same as Figure 2 but computed for flood events of rainfall (unit; mm/day), surface pressure (unit; hPa) and surface temperature (unit; °C).
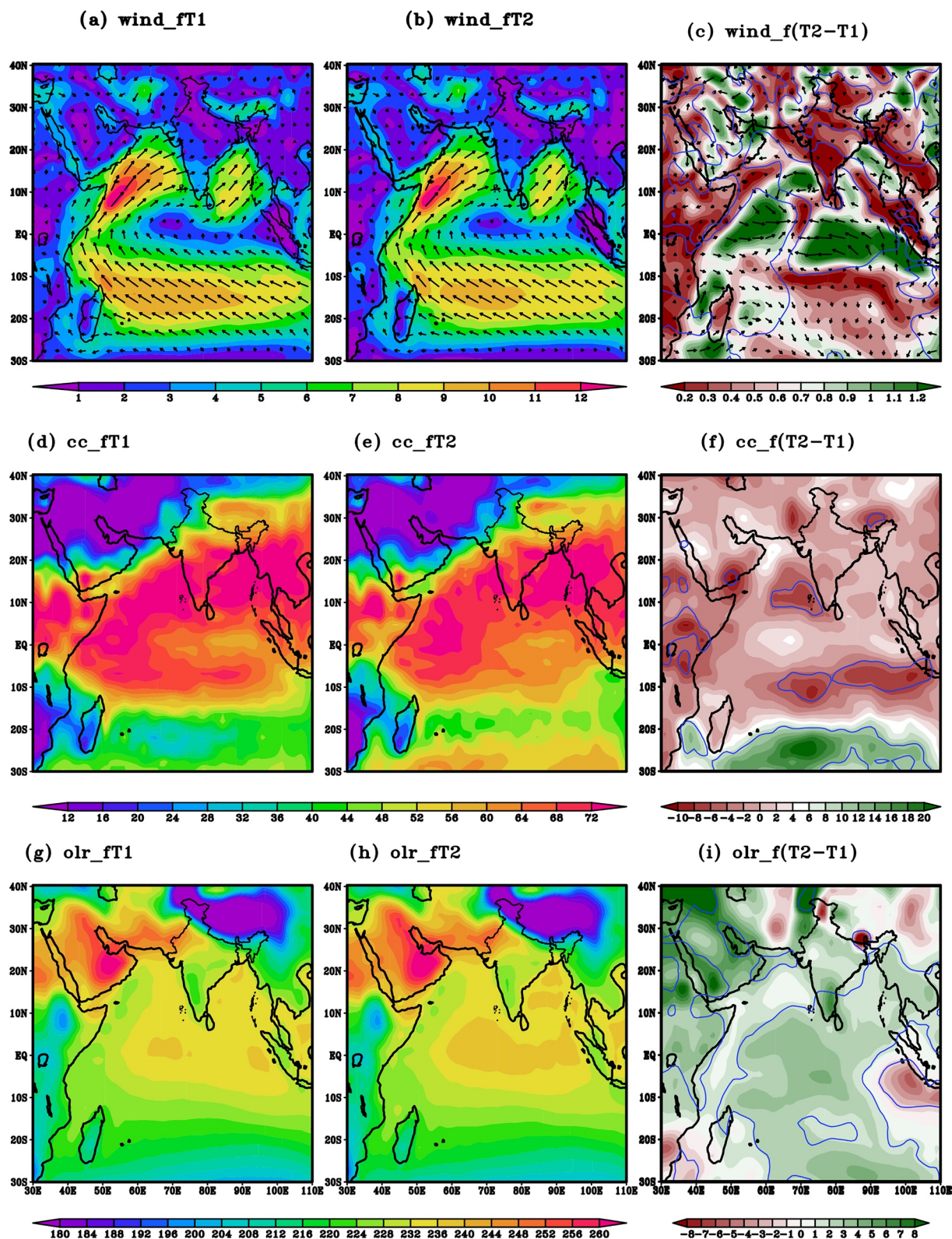
Figure 7. (a–i) Same as Figure 2 but computed for flood events of wind vector (unit; m/s), cloud cover (unit; %) and outgoing longwave radiation (W/m²).
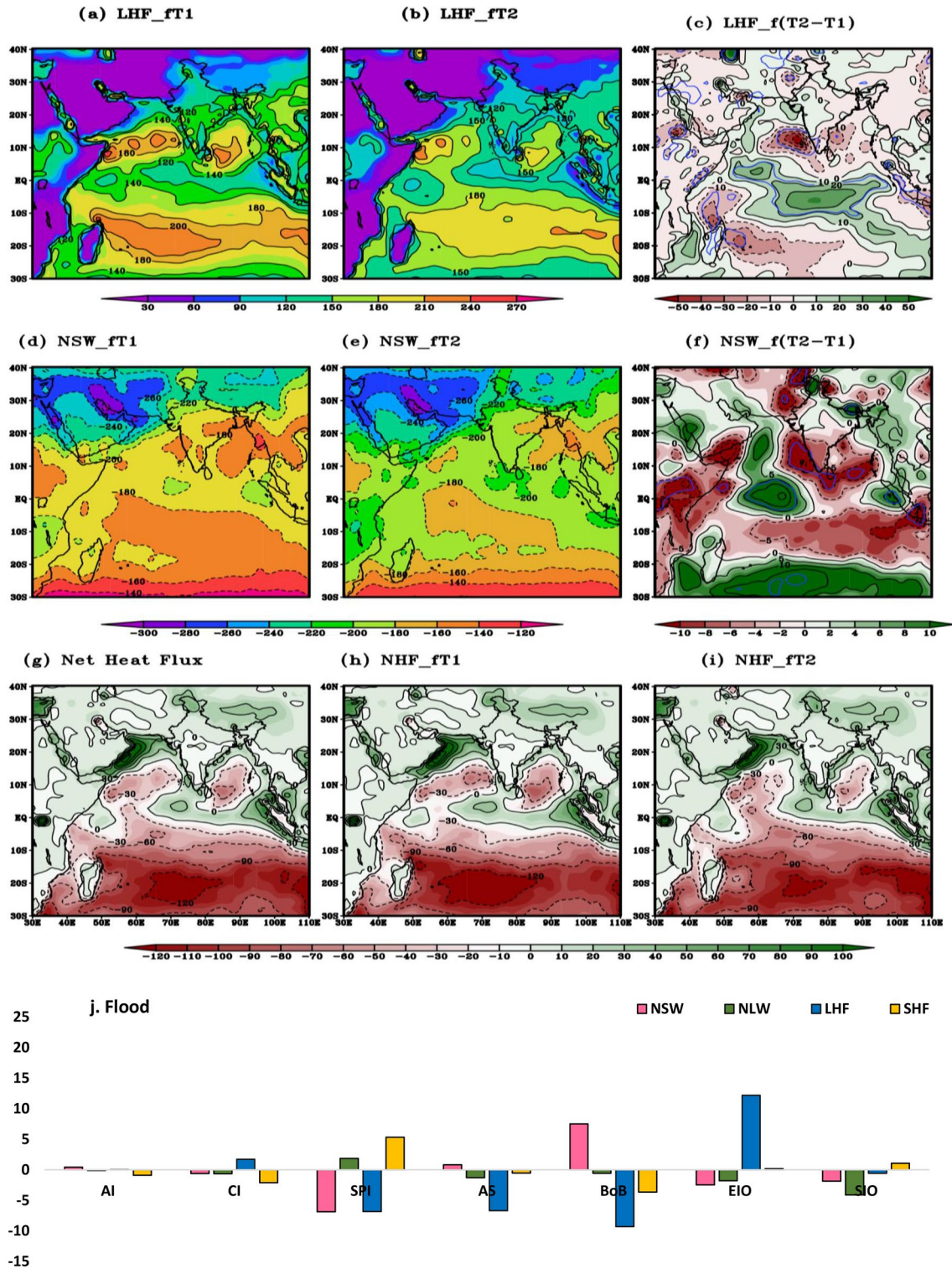
Figure 8. (a–i) Same as Figure 4 but computed for flood events of latent heat flux (W/m²), net Incoming shortwave radiation (W/m²) and net heat flux (W/m²) (j) temporal tricadal departure of land and oceanic surface fluxes over selected regions during flood event.

tricade (T2) the LHF values are less over earlier mentioned oceanic regions which is also can be seen in the difference pattern (T2-T1) with values ranging −30 to −40 W/m² (Figures 8b and 8c). Contrary to that, a huge enhancement (20–50 W/m²) in LHF has been observed over EIO region. Similarly, the distribution for NSWRF is found to be minimum over EIO, AS, BoB and most of the Indian landmass. The fluctuations of NSWRF during

the monsoonal flood events in T1 and T2 remarkably comparable over CI, and WI (200–220 W/m²) whereas differing over SPI, NEI, and upper NI (200 W/m²) (Figure 8d). However, a declining pattern of NSWRF over oceanic regions have been observed during T1 and T2 (Figures 8d and 8e). An enhancement over upper SIO (0.3–0.4 W/m²), EAS, WGs, SPI, and some parts of CI although a decline in NSWRF has been observed over lower SIO, WAS, NI, and NE regions and eight statistically significant with student's t-test at 95% level in blue contour line (Figure 8f). The distribution of NHF is similar over most of the oceanic (−60 to −100 W/m²) and Indian landmass (10–20 W/m²) regions during past and recent flood years (Figures 8g–8i). However, larger negative distribution (−110 to −120 W/m²) of NHF can be noticed over SIO during past as compared to the recent epochs. The temporal differences (recent to past) in flood events for different surface fluxes over seven selected regions are depicted in Figure 8j. The large variations of surface fluxes moreover oceanic region (AS, BoB, EIO) than land region except SPI. The NSWRF value shows significant negative departure over SPI, EIO, SIO (below −10 W/m²) for flood event but on the other hand the positive departure is concentrated only over BoB about 7 W/m² (Figure 8j). However, the significant positive departure of LHF over EIO (12 W/m²) while significant negative departure observed over SPI, AS, BoB (−5 W/m²), it is clearly observed that latent heating decreases in recent tricade during monsoonal flood events.

3.6. Spatiotemporal Variation of Thermodynamic Features During Flood Events of AISM

The spatial distribution of DSE, MSE, and VIMFC during the flood episodes in past, recent and their epochal differences have been depicted in Figures 9a–9i. The variations in DSE have been found to be minimum over SIO (290–295 kJ/kg) which further increases over EIO (298–302 kJ/kg), AS, BoB, SI, SPI (302–304 kJ/kg), WI, NI, NEI (304–308 kJ/kg) regions. There is an enhancement of DSE over almost the entire region (0.2–1.0 kJ/kg) except some parts of southern AS, Mascarene and eastern SIO regions during the recent tricade and significant above 95% confidence level (Figure 9c). Similarly, the spatial variation of MSE for flood episodes depicted in Figures 9d–9f. There is also enhancement of MSE in recent tricade over most of the land and oceanic regions except eastern SIO. Further spatial variation of VIMFC depicted convergence (positive VIMFC) and divergence (negative VIMFC) region during composite of monsoonal flood events (Figures 9g–9i). There are positive VIMFC observed over oceanic region such that western side of SIO, EIO, AS, and BoB further over land region as some parts of WI, CI, NI, and NEI (0.02–0.08 × 10⁻⁵ kg/m²s) (Figure 9i). Also, negative changes of VIMFC observed over some parts of SIO (−0.02 to −0.06 × 10⁻⁵ kg/m²s), southern AS, SPI, some parts of southern BOB, and some parts of WI (−0.02 to −0.05 × 10⁻⁵ kg/m²s). The epochal changes of VIMFC follows the oscillation pattern from south to northward propagation similar as rainfall path Figure 6c. Several supporting reason behind that VIMFC anomalies are coherent with rainfall during ISM season (Li et al., 2018; Muhammad & Lubis, 2022).

3.7. Contrasting Dynamical and Thermodynamical Features of Drought and Flood Events in Past and Recent Monsoonal Epochs During ISM Season

There are some positive rainfall anomalies (from past to recent monsoonal drought and flood events) observed over WI, CI, some parts of NI, and NEI supporting strengthening in rainfall (Figures 2c and 5c). It is clearly observed in recent tricades of all Indian drought events, the spatial pattern of surface pressure and temperature having more over WSIO, WAS supports the westward shifting of monsoonal rainfall. By the comparison of monsoonal drought events with flood events, there is contrasting nature observed in wind vectors, CC, as well as OLR. From the past to recent tricades of wind pattern in monsoonal flood events more strengthening than monsoonal drought events due to more moisture energy flux (Raju et al., 2002). Similarly, in recent tricades the spatial distribution of CC more over EIO, while less over SIO in flood events than drought events during ISM. Along with that the past and recent monsoonal flood events having more OLR over land and oceanic than monsoonal drought events support more convection heating with excess rainfall. There are diminishing in LHF from past to recent monsoonal drought events over EAS, BoB, WGs, some parts of SPI, and the upper NI region while increase in strength over EIO, WAS, CI, WI, some parts of lower SPI, and NEI region. More convection heating over EIO, WAS, and CI region in all India composite drought events than flood events during monsoon season due to having more latent heating. Furthermore, there is an increase in NSWRF from past to recent tricades during monsoonal drought and flood events over WAS, lower SIO, and EIO but more strengthening in magnitude during drought events. In contrast, more weakening in NSWRF over some parts of CI, SPI, WGs, AS, BoB, and upper SIO region for drought events than flood events during monsoon season. In recent tricades monsoonal drought (flood) events are more severe due to more (less) NSWRF. Similarly, the spatial distribution of NHF from past to recent tricades as well as all India drought (flood) events during monsoon season, less
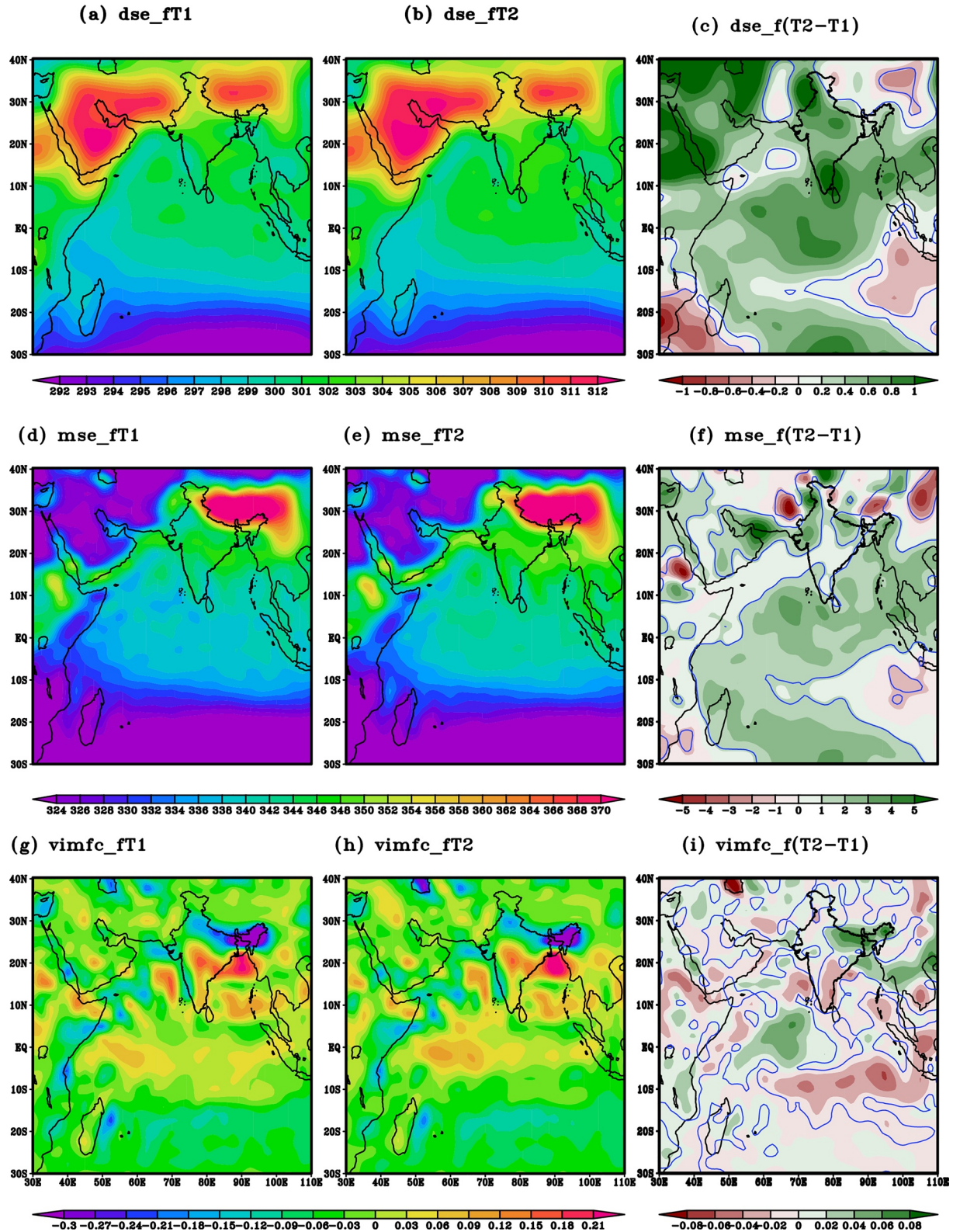
Figure 9. (a–i) Same as Figure 2 but computed for flood events of dry static energy (kJ/kg), moist static energy (kJ/kg) and vertically integrated moisture flux convergence (10^{-5}kgm^{-2}s^{-1}).

negative flux found over AS, BoB, and EIO regions and more negative NHF observed over SIO. Further, some positive values of NHF were also observed over EAS, WGs, Western BoB, and some parts of EIO during the recent tricade of monsoonal flood events. While from past to recent monsoonal drought events, positive (negative) NHF is observed over land and adjoining region (oceanic region). The major source of energy for water vapor is the advection of moisture from the AS through WGs over all Indian regions during the monsoon season (Mirza, 2011; Neena et al., 2011; Pathak et al., 2017). The NSWRF value represents significant positive departure over SPI and BoB (15 W/m^2) for drought event but on the other hand during flood event this departure is observed only over BoB region (7 W/m^2) which implies the frequency of drought in recent tricade declined but the raised in NSWRF have been severe drought than flood. The spatial variation of thermodynamic features such as DSE, MSE, and VIMFC are associated with surface fluxes and play a significant role for the rainfall variability during ISM season. A slightly decreasing pattern of DSE and MSE observed over western side of SIO, EIO, and AS (−0.2 to −0.5 kJ/kg for DSE; −1 to −2 kJ/kg for MSE; Figures 5c and 5f) during monsoonal drought events. Meanwhile the epochal differences (from past to recent tricade) of DSE and MSE slightly decreases over eastern side of SIO and Mascarene region during composite flood events of ISM (−0.2 to −0.6 kJ/kg for DSE; −1 to −2 kJ/kg for MSE; Figures 9c and 9f). In contrast, the rest part of the Indian region having positive MSE & DSE observed for composite drought and flood events. The analysis of composite monsoonal drought and flood episodes of VIMFC represents the flux convergence of moisture exist over the land and oceanic region with a maximum value concentrated over the BoB, AS, adjoining region of SPI, and EIO with the order of 0.03–0.2 × 10^{-5} kg/m^{2}s. From Figures 2c and 6c, it is observed that epochal differences of VIMFC consistent with flood (drought) rainfall differences from past to recent tricade during ISM season.

4. Conclusions

The enhancement of rainfall is supported by the positive rainfall anomalies (from previous to recent monsoonal drought (flood) episodes) found over significant land regions (Figures 2c and 5c). Although the negative rainfall anomaly over the AS, BoB, SPI, and upper NI region demonstrates decreasing rainfall during past tricadal monsoonal drought events. The spatiotemporal pattern of surface pressure and temperature, which has higher influence over WSIO, WAS, indicates the westward shifting of monsoonal rainfall in recent tricades of all Indian drought episodes. When monsoonal drought and flood episodes are compared, distinct patterns in wind directions, CC, and OLR perceived. By the comparison of epochal changes of all India flood and drought events, more convective heating occurred over the EIO, and WAS region due to more latent heating and incoming solar radiation in recent epoch and these changes are statistically significant above 95% confidence level. The increase (decrease) NSWRF during the recent tricade, the occurrence of monsoonal drought (flood) have become more severe. The NSWRF value shows significant positive departure over SPI and BoB (>15 W/m^2) for drought events but on the other hand during flood event this departure is concentrated only over BoB region in the range of 7 W/m^2 which implies about the frequency of drought in recent tricade are low but the elevated value of NSWRF would cause more severe drought than flood. The positive NHF over land region indicates a heating region (enhancing incoming radiation with diminishing outgoing radiation, source region) although negative NHF over oceanic region indicates the cooling (sinking) region. The undulating behavior of convective heating is associated with a significantly changing pattern of surface heat fluxes and thermodynamic features observed in composite monsoonal drought and flood episodes. DSE & MSE variations directly linked to the surface energy fluxes and playing a secondary role in rainfall variability during ISM season. The epochal differences of VIMFC are persistent with flood (drought) rainfall anomaly. There are decreasing pattern of VIMFC concentrated over SIO, southern AS, southern BoB, SPI, and some parts of WI (−0.03 to −0.09 × 10^{-5} kg/m^{2}s) manifests drought are more severe in recent tricade than flood events. As a result, major asymmetric ISM phenomena like drought and flood events could have a severe effect on moisture availability, crop growth and water resource management across India.

Data Availability Statement

The India Meteorological Department (IMD)'s observed daily gridded rainfall data (IMD4) at resolution (0.25° × 0.25°) is available through the "Data Supply Portal" on payment basis (http://dsp.imdpune.gov.in/). The NCEP reanalysis data (rainfall, surface pressure, surface temperature, wind (zonal & meridional), CC, LHF, NLWRF, NSWRF, and SHF) used in this paper are available at http://www.cdc.noaa.gov/cdc/data.ncep.reanalysis.surface.html.

References

Annamalai, H., Hafner, J., Sooraj, K. P., & Pillai, P. (2013). Global warming shifts the monsoon circulation, drying South Asia. *Journal of Climate*, *26*(9), 2701–2718. https://doi.org/10.1175/jcli-d-12-00208.1

Ashok, K., & Tejavath, C. T. (2019). The Indian summer monsoon rainfall and ENSO. *Mausam*, *70*(3), 443–452. https://doi.org/10.54302/mausam.v70i3.224

Bhalme, H. N., & Mooley, D. A. (1980). Large-scale droughts/floods and monsoon circulation.

Bhat, G. S. (2002). Near-surface variations and surface fluxes over the northern Bay of Bengal during the 1999 Indian summer monsoon. *Journal of Geophysical Research*, *107*(D17), ACL6-1–ACL6-19. https://doi.org/10.1029/2001jd000382

Bhatla, R., Gyawali, B., Mall, R. K., & Raju, P. V. S. (2013). Study of possible linkage of PDO with Indian summer monsoon in relation to QBO. *Vayumandal*, *39*(1–2), 40–45.

Bhatla, R., Maurya, A., Sinha, P., Verma, S., & Pant, M. (2022). Assessment of climate change of different meteorological state variables during Indian summer monsoon season. *Journal of Earth System Science*, *131*(2), 1–23. https://doi.org/10.1007/s12040-022-01878-1

Bhatla, R., Raju, P. V. S., Mohanty, U. C., Madan, O. P., & Mall, R. K. (2011). Study of energy fluxes over the Indian Ocean prior and during the summer monsoon. *Marine Geodesy*, *34*(2), 119–137. https://doi.org/10.1080/01490419.2011.571557

Bhatla, R., Sharma, S., Verma, S., & Gyawali, B. (2020). Impact of Pacific Decadal Oscillation in relation to QBO on Indian summer monsoon rainfall. *Arabian Journal of Geosciences*, *13*(22), 1–9. https://doi.org/10.1007/s12517-020-06225-6

Bingyi, W. (2005). Weakening of Indian summer monsoon in recent decades. *Advances in Atmospheric Sciences*, *22*(1), 21–29. https://doi.org/10.1007/bf02930866

Boos, W. R., & Emanuel, K. A. (2009). Annual intensification of the Somali jet in a quasi-equilibrium framework: Observational composites. *Quarterly Journal of the Royal Meteorological Society: A Journal of the Atmospheric Sciences, Applied Meteorology and Physical Oceanography*, *135*(639), 319–335. https://doi.org/10.1002/qj.388

Cadet, D. L., & Diehl, B. C. (1984). Interannual variability of surface fields over the Indian Ocean during recent decades. *Monthly Weather Review*, *112*(10), 1921–1935. https://doi.org/10.1175/1520-0493(1984)112<1921:ivosfo>2.0.co;2

Chakraborty, A., & Agrawal, S. (2017). Role of west Asian surface pressure in summer monsoon onset over central India. *Environmental Research Letters*, *12*(7), 074002. https://doi.org/10.1088/1748-9326/aa76ca

Dhanya, C. T., & Nagesh Kumar, D. (2009). Data mining for evolution of association rules for droughts and floods in India using climate inputs. *Journal of Geophysical Research*, *114*(D2), D02102. https://doi.org/10.1029/2008jd010485

Ding, Y. (2007). The variability of the Asian summer monsoon. *Journal of the Meteorological Society of Japan. Ser. II*, *85*(0), 21–54. https://doi.org/10.2151/jmsj.85b.21

Dirmeyer, P. A. (1998). Land-sea geometry and its effect on monsoon circulations. *Journal of Geophysical Research*, *103*(D10), 11555–11572. https://doi.org/10.1029/98jd00802

Fu, X., Wang, B., & Li, T. (2002). Impacts of air–sea coupling on the simulation of mean Asian summer monsoon in the ECHAM4 model. *Monthly Weather Review*, *130*(12), 2889–2904. https://doi.org/10.1175/1520-0493(2002)130<2889:ioasco>2.0.co;2

Gadgil, S. (2000). Monsoon–ocean coupling. *Current Science*, 309–322.

Gadgil, S., & Joseph, P. V. (2003). On breaks of the Indian monsoon. *Journal of Earth System Science*, *112*(4), 529–558. https://doi.org/10.1007/bf02709778

Gadgil, S., Vinayachandran, P. N., & Francis, P. A. (2003). Droughts of the Indian summer monsoon: Role of clouds over the Indian Ocean. *Current Science*, 1713–1719.

Ghosh, S. K., Pant, M. C., & Dewan, B. N. (1978). Influence of the Arabian Sea on the Indian summer monsoon. *Tellus*, *30*(2), 117–125. https://doi.org/10.1111/j.2153-3490.1978.tb00825.x

Goswami, B. N. (2006). The Asian monsoon: Interdecadal variability. In *The Asian monsoon* (pp. 295–327). Springer.

Goswami, B. N., Ajayamohan, R. S., Xavier, P. K., & Sengupta, D. (2003). Clustering of synoptic activity by Indian summer monsoon intraseasonal oscillations. *Geophysical Research Letters*, *30*(8), 1431. https://doi.org/10.1029/2002gl016734

Goswami, B. N., & Ajaymohan, R. S. (2001). Intra-seasonal oscillations and predictability of the Indian summer monsoon. *Proceedings of Indian National Science Academy*, *67*(3), 369–383.

Goswami, B. N., & Chakravorty, S. (2017). Dynamics of the Indian summer monsoon climate. In *Oxford research encyclopedia of climate science*.

Goswami, B. N., Kripalani, R. H., Borgaonkar, H. P., & Preethi, B. (2016). Multi-decadal variability in Indian summer monsoon rainfall using proxy data. In *Climate change: Multidecadal and beyond* (pp. 327–345).

Goswami, B. N., & Xavier, P. K. (2003). Potential predictability and extended range prediction of Indian summer monsoon breaks. *Geophysical Research Letters*, *30*(18), 1966. https://doi.org/10.1029/2003gl017810

Gu, Y., Liu, H., Traoré, D. D., & Huang, C. (2020). ENSO-related droughts and ISM variations during the last millennium in tropical southwest China. *Climate Dynamics*, *54*(1), 649–659. https://doi.org/10.1007/s00382-019-05019-1

Guhathakurta, P., & Rajeevan, M. (2008). Trends in the rainfall pattern over India. *International Journal of Climatology: A Journal of the Royal Meteorological Society*, *28*(11), 1453–1469. https://doi.org/10.1002/joc.1640

Hrudya, P. H., Varikoden, H., & Vishnu, R. (2021). A review on the Indian summer monsoon rainfall, variability and its association with ENSO and IOD. *Meteorology and Atmospheric Physics*, *133*(1), 1–14. https://doi.org/10.1007/s00703-020-00734-5

Joseph, P. V., & Simon, A. (2005). Weakening trend of the southwest monsoon current through peninsular India from 1950 to the present. *Current Science*, 687–694.

Joseph, P. V., Sooraj, K. P., & Rajan, C. K. (2006). The summer monsoon onset process over South Asia and an objective method for the date of monsoon onset over Kerala. *International Journal of Climatology: A Journal of the Royal Meteorological Society*, *26*(13), 1871–1893. https://doi.org/10.1002/joc.1340

Joseph, S., Sahai, A. K., & Goswami, B. N. (2009). Eastward propagating MJO during boreal summer and Indian monsoon droughts. *Climate Dynamics*, *32*(7), 1139–1153. https://doi.org/10.1007/s00382-008-0412-8

Kalnay, E., Kanamitsu, M., Kistler, R., Collins, W., Deaven, D., Gandin, L., et al. (1996). The NCEP/NCAR 40–year reanalysis project. *Bulletin of the American Meteorological Society*, *77*(3), 437–471. https://doi.org/10.1175/1520-0477(1996)077<0437:tnyrp>2.0.co;2

Kothawale, D. R., Munot, A. A., & Borgaonkar, H. P. (2008). Temperature variability over the Indian Ocean and its relationship with Indian summer monsoon rainfall. *Theoretical and Applied Climatology*, *92*(1), 31–45. https://doi.org/10.1007/s00704-006-0291-z

Krishna, K. M., & Rao, S. R. (2008). Study of Indian summer monsoon rainfall on decadal scales vis-à-vis circulation patterns. *Canadian Journal of Pure and Applied Sciences*, *441*.

Krishnamurthy, V., & Goswami, B. N. (2000). Indian monsoon–ENSO relationship on interdecadal timescale. *Journal of Climate*, *13*(3), 579–595. https://doi.org/10.1175/1520-0442(2000)013<0579:imeroi>2.0.co;2

Krishnamurthy, V., & Shukla, J. (2007). Intraseasonal and seasonally persisting patterns of Indian monsoon rainfall. *Journal of Climate*, *20*(1), 3–20. https://doi.org/10.1175/JCLI3981.1

Krishnan, R., Sabin, T. P., Ayantika, D. C., Kitoh, A., Sugi, M., Murakami, H., et al. (2013). Will the South Asian monsoon overturning circulation stabilize any further? *Climate Dynamics*, *40*(1), 187–211. https://doi.org/10.1007/s00382-012-1317-0

Levine, R. C., & Turner, A. G. (2012). Dependence of Indian monsoon rainfall on moisture fluxes across the Arabian Sea and the impact of coupled model sea surface temperature biases. *Climate Dynamics*, *38*(11), 2167–2190. https://doi.org/10.1007/s00382-011-1096-z

Li, L., Schmitt, R. W., & Ummenhofer, C. C. (2018). The role of the subtropical North Atlantic water cycle in recent US extreme precipitation events. *Climate Dynamics*, *50*(3), 1291–1305. https://doi.org/10.1007/s00382-017-3685-y

Mahto, S. S., & Mishra, V. (2020). Dominance of summer monsoon flash droughts in India. *Environmental Research Letters*, *15*(10), 104061. https://doi.org/10.1088/1748-9326/abaf1d

Malik, A., & Brönnimann, S. (2018). Factors affecting the inter-annual to centennial timescale variability of Indian summer monsoon rainfall. *Climate Dynamics*, *50*(11), 4347–4364. https://doi.org/10.1007/s00382-017-3879-3

May, W. (2004). Potential future changes in the Indian summer monsoon due to greenhouse warming: Analysis of mechanisms in a global time-slice experiment. *Climate Dynamics*, *22*(4), 389–414. https://doi.org/10.1007/s00382-003-0389-2

Mirza, M. (2011). Climate change, flooding in South Asia and implications. *Regional Environmental Change*, *11*(1), 95–107. https://doi.org/10.1007/s10113-010-0184-7

Mishra, A. K., Dwivedi, S., Di Sante, F., & Coppola, E. (2020). Thermodynamical properties associated with the Indian summer monsoon rainfall using a regional climate model. *Theoretical and Applied Climatology*, *141*(1), 587–599. https://doi.org/10.1007/s00704-020-03237-w

Mishra, V., Aadhar, S., Asoka, A., Pai, S., & Kumar, R. (2016). On the frequency of the 2015 monsoon season drought in the Indo-Gangetic Plain. *Geophysical Research Letters*, *43*(23), 12–102. https://doi.org/10.1002/2016gl071407

Mishra, V., Shah, R., Azhar, S., Shah, H., Modi, P., & Kumar, R. (2018). Reconstruction of droughts in India using multiple land-surface models (1951–2015). *Hydrology and Earth System Sciences*, *22*(4), 2269–2284. https://doi.org/10.5194/hess-22-2269-2018

Mohanty, P. K., & Dash, S. K. (1995). Variability of surface fields in different branches of monsoon. *Mausam*, *46*(3), 313–324. https://doi.org/10.54302/mausam.v46i3.3291

Mohanty, U. C., & Mohan Kumar, V. (1990). A study on energy fluxes in the surface boundary layer of the Indian seas during different epochs of the Asian summer monsoon. *Atmospheric Environment*, *24*(4), 823–828. https://doi.org/10.1016/0960-1686(90)90283-s

Mohanty, U. C., & Ramesh, K. J. (1993). Characteristics of certain surface meteorological parameters in relation to the interannual variability of Indian summer monsoon. *Proceedings of the Indian Academy of Sciences - Earth & Planetary Sciences*, *102*(1), 73–87. https://doi.org/10.1007/bf02839183

Mohanty, U. C., Ramesh, K. J., Kumar, N. M., & Potty, K. V. J. (1994). Variability of the Indian summer monsoon in relation to oceanic heat budget over the Indian seas. *Dynamics of Atmospheres and Oceans*, *21*(1), 1–22. https://doi.org/10.1016/0377-0265(94)90023-x

Mohanty, U. C., Ramesh, K. J., & Pant, M. C. (1996). Certain seasonal characteristic features of oceanic heat budget components over the Indian seas in relation to the summer monsoon activity over India. *International Journal of Climatology*, *16*(3), 243–264. https://doi.org/10.1002/(sici)1097-0088(199603)16:3<243::aid-joc2>3.0.co;2-b

Mooley, D. A., & Parthasarathy, B. (1984). Fluctuations in all-India summer monsoon rainfall during 1871–1978. *Climatic Change*, *6*(3), 287–301. https://doi.org/10.1007/bf00142477

MP, S. (1983). A study of heat and moisture budget over the Arabian Sea and their role in the onset and maintenance of summer monsoon. *Journal of the Meteorological Society of Japan. Series II*, *61*(2), 208–221.

Muhammad, F. R., & Lubis, S. W. (2022). Impacts of the boreal summer intraseasonal oscillation (BSISO) on precipitation extremes in Indonesia. *International Journal of Climatology*. https://doi.org/10.1002/joc.7934

Naidu, C. V., Krishna, K. M., Rao, S. R., Kumar, O. B., Durgalakshmi, K., & Ramakrishna, S. S. V. S. (2011). Variations of Indian summer monsoon rainfall induce the weakening of easterly jet stream in the warming environment? *Global and Planetary Change*, *75*(1–2), 21–30. https://doi.org/10.1016/j.gloplacha.2010.10.001

Nair, P. J., Varikoden, H., Francis, P. A., Chakraborty, A., & Pandey, P. C. (2021). Atmospheric moisture as a proxy for the ISMR variability and associated extreme weather events. *Environmental Research Letters*, *16*(1), 014045. https://doi.org/10.1088/1748-9326/abcfe0

Nanjundiah, R. S., & Srinivasan, J. (1999). Anomalies of precipitable water vapor and vertical stability during El Nino. *Geophysical Research Letters*, *26*(1), 95–98. https://doi.org/10.1029/1998gl900254

Narapusetty, B., Murtugudde, R., Wang, H., & Kumar, A. (2016). Ocean–atmosphere processes driving Indian summer monsoon biases in CFSv2 hindcasts. *Climate Dynamics*, *47*(5), 1417–1433. https://doi.org/10.1007/s00382-015-2910-9

Neelin, J. D. (2007). Moist dynamics of tropical convection zones in monsoons, teleconnections, and global warming. *The Global Circulation of the Atmosphere*, *267*, 301.

Neena, J. M., Suhas, E., & Goswami, B. N. (2011). Leading role of internal dynamics in the 2009 Indian summer monsoon drought. *Journal of Geophysical Research*, *116*(D13), D13103. https://doi.org/10.1029/2010JD015328

Parthasarathy, B., & Mooley, D. A. (1978). Some features of a long homogeneous series of Indian summer monsoon rainfall. *Monthly Weather Review*, *106*(6), 771–781. https://doi.org/10.1175/1520-0493(1978)106<0771:sfoalh>2.0.co;2

Parthasarathy, B., Munot, A. A., & Kothawale, D. R. (1994). All-India monthly and seasonal rainfall series: 1871–1993. *Theoretical and Applied Climatology*, *49*(4), 217–224. https://doi.org/10.1007/bf00867461

Pathak, A., Ghosh, S., Martinez, J. A., Dominguez, F., & Kumar, P. (2017). Role of oceanic and land moisture sources and transport in the seasonal and interannual variability of summer monsoon in India. *Journal of Climate*, *30*(5), 1839–1859. https://doi.org/10.1175/jcli-d-16-0156.1

Pillai, P. A., & Sahai, A. K. (2014). Moist dynamics of active/break cycle of Indian summer monsoon rainfall from NCEPR2 and MERRA reanalysis. *International Journal of Climatology*, *34*(5), 1429–1444. https://doi.org/10.1002/joc.3774

Rahul, S., & Gnanaseelan, C. (2016). Can large scale surface circulation changes modulate the sea surface warming pattern in the Tropical Indian Ocean? *Climate Dynamics*, *46*(11), 3617–3632. https://doi.org/10.1007/s00382-015-2790-z

Rajeevan, M., De, U. S., & Prasad, R. K. (2000). Decadal variation of sea surface temperatures, cloudiness and monsoon depressions in the north Indian Ocean. *Current Science*, *79*(3), 283–285.

Rajeevan, M., Gadgil, S., & Bhate, J. (2010). Active and break spells of the Indian summer monsoon. *Journal of Earth System Science*, *119*(3), 229–247. https://doi.org/10.1007/s12040-010-0019-4

Rajesh, P. V., & Goswami, B. N. (2020). Four-dimensional structure and sub-seasonal regulation of the Indian summer monsoon multi-decadal mode. *Climate Dynamics*, *55*(9), 2645–2666. https://doi.org/10.1007/s00382-020-05407-y

Raju, P. V. S., Mohanty, U. C., Rao, P. L. S., & Bhatla, R. (2002). The contrasting features of Asian summer monsoon during surplus and deficient rainfall over India. *International Journal of Climatology: A Journal of the Royal Meteorological Society*, *22*(15), 1897–1914. https://doi.org/10.1002/joc.855

Ramesh Kumar, M. R., Sankar, S., Fennig, K., Pai, D. S., & Schulz, J. (2005). Air Sea Interaction over the IO during the contrasting monsoon years 2002 and 2003. *Geophysical Research Letters*, *32*(14), L14821. https://doi.org/10.1029/2005GL022587

Roxy, M. K., Ritika, K., Terray, P., & Masson, S. (2014). The curious case of Indian Ocean warming. *Journal of Climate*, *27*(22), 8501–8509. https://doi.org/10.1175/jcli-d-14-00471.1

Roxy, M. K., Ritika, K., Terray, P., Murtugudde, R., Ashok, K., & Goswami, B. N. (2015). Drying of Indian subcontinent by rapid Indian Ocean warming and a weakening land-sea thermal gradient. *Nature Communications*, *6*(1), 1–10. https://doi.org/10.1038/ncomms8423

Sahana, A. S., Ghosh, S., Ganguly, A., & Murtugudde, R. (2015). Shift in Indian summer monsoon onset during 1976/1977. *Environmental Research Letters*, *10*(5), 054006. https://doi.org/10.1088/1748-9326/10/5/054006

Samson, G., Masson, S., Durand, F., Terray, P., Berthet, S., & Jullien, S. (2017). Roles of land surface albedo and horizontal resolution on the Indian summer monsoon biases in a coupled ocean–atmosphere tropical-channel model. *Climate Dynamics*, *48*(5), 1571–1594. https://doi.org/10.1007/s00382-016-3161-0

Shukla, J. (1987). Interannual variability of monsoons. *Monsoons*, *14*, 399–464.

Sikka, D. R. (1980). Some aspects of the large scale fluctuations of summer monsoon rainfall over India in relation to fluctuations in the planetary and regional scale circulation parameters. *Proceedings of the Indian Academy of Sciences—Earth & Planetary Sciences*, *89*(2), 179–195. https://doi.org/10.1007/bf02913749

Sikka, D. R., & Gadgil, S. (1978). Large–scale rainfall over India during the summer monsoon and its relation of the lower and upper tropospheric vorticity. *Indian Journal of Meteorology, Hydrology and Geophysics*, *29*(1), 219–231. https://doi.org/10.54302/mausam.v29i1.2881

Sikka, D. R., & Gadgil, S. (1980). On the maximum cloud zone and the ITCZ over Indian longitudes during the southwest monsoon. *Monthly Weather Review*, *108*(11), 1840–1853. https://doi.org/10.1175/1520-0493(1980)108<1840:otmcza>2.0.co;2

Singh, P., & Borah, B. (2013). Indian summer monsoon rainfall prediction using artificial neural network. *Stochastic Environmental Research and Risk Assessment*, *27*(7), 1585–1599. https://doi.org/10.1007/s00477-013-0695-0

Sinha, A., Kathayat, G., Cheng, H., Breitenbach, S. F., Berkelhammer, M., Mudelsee, M., et al. (2015). Trends and oscillations in the Indian summer monsoon rainfall over the last two millennia. *Nature Communications*, *6*(1), 1–8. https://doi.org/10.1038/ncomms7309

Sujith, K., Saha, S. K., Pokhrel, S., Hazra, A., & Chaudhari, H. S. (2017). The dominant modes of recycled monsoon rainfall over India. *Journal of Hydrometeorology*, *18*(10), 2647–2657. https://doi.org/10.1175/jhm-d-17-0082.1

Swain, D., Rahman, S. H., & Ravichandran, M. (2009). Comparison of NCEP turbulent heat fluxes with in situ observations over the southeastern Arabian Sea. *Meteorology and Atmospheric Physics*, *104*(3), 163–175. https://doi.org/10.1007/s00703-009-0023-x

Todmal, R. S., Koteswara Rao, K., Ingle, S., & Korade, M. S. (2022). Impact of southern oscillation and Indian Ocean Dipole on rainfall variability over India: Trends and interlinkages during 1871–2017. *Meteorology and Atmospheric Physics*, *134*(6), 1–19. https://doi.org/10.1007/s00703-022-00936-z

Trenberth, K. E., & Guillemot, C. J. (1998). Evaluation of the atmospheric moisture and hydrological cycle in the NCEP/NCAR reanalyses. *Climate Dynamics*, *14*(3), 213–231. https://doi.org/10.1007/s003820050219

Trenberth, K. E., Hurrell, J. W., & Stepaniak, D. P. (2006). The Asian monsoon: Global perspectives. In *The Asian monsoon* (pp. 67–87). Springer.

Trenberth, K. E., & Stepaniak, D. P. (2004). The flow of energy through the Earth's climate system. *Quarterly Journal of the Royal Meteorological Society: A Journal of the Atmospheric Sciences, Applied Meteorology and Physical Oceanography*, *130*(603), 2677–2701. https://doi.org/10.1256/qj.04.83

Turner, A. G., & Annamalai, H. (2012). Climate change and the South Asian summer monsoon. *Nature Climate Change*, *2*(8 Guhathakurta), 587–595. https://doi.org/10.1038/nclimate1495

Vaid, B. H., & Kripalani, R. H. (2021). Strikingly contrasting Indian monsoon progressions during 2013 and 2014: Role of Western Tibetan Plateau and the South China Sea. *Theoretical and Applied Climatology*, *144*(3), 1131–1140. https://doi.org/10.1007/s00704-021-03590-4

Varikoden, H., Revadekar, J. V., Choudhary, Y., & Preethi, B. (2015). Droughts of Indian summer monsoon associated with El Niño and Non-El Niño years. *International Journal of Climatology*, *35*(8), 1916–1925. https://doi.org/10.1002/joc.4097

Vishnu, S., Boos, W. R., Ullrich, P. A., & O'Brien, T. A. (2020). Assessing historical variability of South Asian monsoon lows and depressions with an optimized tracking algorithm. *Journal of Geophysical Research: Atmospheres*, *125*(15), e2020JD032977. https://doi.org/10.1029/2020jd032977

Vishnu, S., Chakraborty, A., & Srinivasan, J. (2022). Why the droughts of the Indian summer monsoon are more severe than the floods. *Climate Dynamics*, *58*(11), 3497–3512. https://doi.org/10.1007/s00382-021-06111-1

Vishnu, S., Francis, P. A., Shenoi, S. S. C., & Ramakrishna, S. S. V. S. (2016). On the decreasing trend of the number of monsoon depressions in the Bay of Bengal. *Environmental Research Letters*, *11*(1), 014011. https://doi.org/10.1088/1748-9326/11/1/014011

Wang, T., Yang, X. Q., Fang, J., Sun, X., & Ren, X. (2018). Role of air–sea interaction in the 30–60-day boreal summer intraseasonal oscillation over the western North Pacific. *Journal of Climate*, *31*(4), 1653–1680. https://doi.org/10.1175/jcli-d-17-0109.1

Webster, P. J. (1981). Monsoons. *Scientific American*, *245*(2), 108–119. https://doi.org/10.1038/scientificamerican0881-108

Webster, P. J., Moore, A. M., Loschnigg, J. P., & Leben, R. R. (1999). Coupled ocean–atmosphere dynamics in the Indian Ocean during 1997–98. *Nature*, *401*(6751), 356–360. https://doi.org/10.1038/43848

Xu, H., Song, Y., Goldsmith, Y., & Lang, Y. (2019). Meridional ITCZ shifts modulate tropical/subtropical Asian monsoon rainfall. *Science Bulletin*, *64*(23), 1737–1739. https://doi.org/10.1016/j.scib.2019.09.025

Xue, F., Wang, H., & He, J. (2004). Interannual variability of Mascarene high and Australian high and their influences on East Asian summer monsoon. *Journal of the Meteorological Society of Japan. Ser. II*, *82*(4), 1173–1186. https://doi.org/10.2151/jmsj.2004.1173

Xue, Y., & Shukla, J. (1993). The influence of land surface properties on Sahel climate. Part 1: Desertification. *Journal of Climate*, *6*(12), 2232–2245. https://doi.org/10.1175/1520-0442(1993)006<2232:tiolsp>2.0.co;2

Yanai, M., & Tomita, T. (1998). Seasonal and interannual variability of atmospheric heat sources and moisture sinks as determined from NCEP–NCAR reanalysis. *Journal of Climate*, *11*(3), 463–482. https://doi.org/10.1175/1520-0442(1998)011<0463:saivoa>2.0.co;2

Yasunari, T. (1979). Cloudiness fluctuations associated with the Northern Hemisphere summer monsoon. *Journal of the Meteorological Society of Japan. Ser. II*, *57*(3), 227–242. https://doi.org/10.2151/jmsj1965.57.3_227